Cell

Glioma Stem Cell Proliferation and Tumor Growth Are Promoted by Nitric Oxide Synthase-2

Christine E. Eyler,[1,2,3] Qiulian Wu,[1] Kenneth Yan,[1] Jennifer M. MacSwords,[1] Devin Chandler-Militello,[5] Katherine L. Misuraca,[2] Justin D. Lathia,[1] Michael T. Forrester,[6] Jeongwu Lee,[1] Jonathan S. Stamler,[7] Steven A. Goldman,[5] Markus Bredel,[10,11] Roger E. McLendon,[4] Andrew E. Sloan,[8] Anita B. Hjelmeland,[1,*] and Jeremy N. Rich[1,9,*]

[1]Department of Stem Cell Biology and Regenerative Medicine, Lerner Research Institute, Cleveland Clinic, Cleveland, OH 44195, USA
[2]Department of Pharmacology and Cancer Biology
[3]Medical Scientist Training Program
[4]Department of Pathology
Duke University Medical Center, Durham, NC 27710, USA
[5]Department of Neurology, University of Rochester Medical Center, Rochester, NY 14642, USA
[6]Department of Medicine, Massachusetts General Hospital, Harvard Medical School, Boston, MA 02114, USA
[7]Institute for Transformative Molecular Medicine and Department of Medicine
[8]Departments of Neurological Surgery, Pathology, and Translational Neuroscience
[9]Department of Molecular Medicine at the Cleveland Clinic Lerner College of Medicine
Case Western Reserve University School of Medicine and University Hospitals, Cleveland, OH 44106, USA
[10]Department of Radiation Oncology, University of Alabama Comprehensive Cancer Center, University of Alabama at Birmingham, Birmingham, AB 35249, USA
[11]Department of Neurosurgery, Neurocenter and Comprehensive Cancer Center, University of Freiburg, D-79106 Freiburg, Germany
*Correspondence: hjelmea@ccf.org (A.B.H.), richj@ccf.org (J.N.R.)
DOI 10.1016/j.cell.2011.06.006

SUMMARY

Malignant gliomas are aggressive brain tumors with limited therapeutic options, and improvements in treatment require a deeper molecular understanding of this disease. As in other cancers, recent studies have identified highly tumorigenic subpopulations within malignant gliomas, known generally as cancer stem cells. Here, we demonstrate that glioma stem cells (GSCs) produce nitric oxide via elevated nitric oxide synthase-2 (NOS2) expression. GSCs depend on NOS2 activity for growth and tumorigenicity, distinguishing them from non-GSCs and normal neural progenitors. Gene expression profiling identified many *NOS2*-regulated genes, including the cell-cycle inhibitor cell division autoantigen-1 (*CDA1*). Further, high *NOS2* expression correlates with decreased survival in human glioma patients, and NOS2 inhibition slows glioma growth in a murine intracranial model. These data provide insight into how GSCs are mechanistically distinct from their less tumorigenic counterparts and suggest that NOS2 inhibition may be an efficacious approach to treating this devastating disease.

INTRODUCTION

Malignant gliomas are highly lethal brain tumors that portend a dismal prognosis for patients. Despite modern surgical and medical treatments, the median survival for glioblastoma patients (WHO grade IV astrocytoma) remains only 14.6 months (Stupp et al., 2005), emphasizing a need for improved therapies. The identification of highly tumorigenic subpopulations within gliomas has fueled enthusiasm for development of novel anti-glioma therapeutics. Due to their high tumorigenic potential and stem cell-like behavior, these cells have earned a variety of names, including tumor-propagating cells or cancer stem cells (CSCs). Unlike the bulk tumor mass, CSCs exhibit sustained self-renewal and produce secondary tumors that recapitulate the parent tumor's features and cellular diversity (Bonnet and Dick, 1997; Galli et al., 2004; Lapidot et al., 1994; Singh et al., 2003; Yuan et al., 2004). The concept of CSCs provides a rational hierarchical explanation for cellular heterogeneity observed within tumors (Reya et al., 2001), which is complementary to stochastic mutations with clonal outgrowths (Shackleton et al., 2009). Regardless of the etiology for tumor heterogeneity, the potent tumor-propagation capacity of CSCs suggests a utility for glioma stem cell (GSC)-directed therapies.

As their name suggests, CSCs share features with nonneoplastic stem cells. Gene expression profiles of GSCs resemble those of embryonic stem cells (Ben-Porath et al., 2008) and nonmalignant neural stem cells (Taylor et al., 2005). Disruption of several stem cell-specific pathways (Bar et al., 2007; Clement et al., 2007; Fan et al., 2006) abrogates CSC proliferation and tumorigenesis, though canonical stem cell signals (e.g., Hedgehog, Notch, and Wnt) are clearly critical to normal stem cell physiology as well (Androutsellis-Theotokis et al., 2006; Reya et al., 2003; Wechsler-Reya and Scott, 1999). Development of strategies that target CSCs while sparing normal stem

cell function is therefore necessary to attain a CSC-selective therapeutic index, a notion that has been supported by studies of leukemic versus hematopoietic stem cells (Yilmaz et al., 2006). In contrast, this concept is relatively unexplored in GSCs versus neural stem cells.

Endogenous nitric oxide (NO) exhibits pleiotropic roles within cancer cells and tumors, and studies employing inhibition or genetic deletion of endogenous NO synthases (NOSs) support a tumor-promoting role for NO (Fukumura et al., 2006; Williams and Djamgoz, 2005). Downstream effects of endogenous NO in cancer include chemotherapeutic resistance (Fetz et al., 2009; Yang et al., 2002), evasion of apoptosis (Engels et al., 2008; Levesque et al., 2003), and enhanced proliferation (Lim et al., 2008). NOS isoforms exhibit heterogeneous expression patterns within glioma cell populations (Bakshi et al., 1998; Cobbs et al., 1995). This heterogeneity may reflect a NOS expression pattern that is restricted to specific glioma subpopulations. This raises the possibility that NOS activity could be unique to GSC subpopulations, as one determinant of glioma heterogeneity relates to the existence of GSCs. Along these lines, studies have suggested a protumorigenic role for NO in gliomas (Charles et al., 2010; Yamaguchi et al., 2002). Endothelial NOS3 localizes near neoplastic cells displaying stem cell markers, and exogenous NO donors support stem cell signaling pathways in murine glioma cells (Charles et al., 2010). However, the therapeutic possibilities of targeting NOS3 in glioma are limited, as previous human trials of nonselective NOS inhibitors (i.e., those with anti-NOS3 activity) resulted in adverse outcomes and increased mortality in sepsis (Alexander et al., 2007; Avontuur et al., 1998; López et al., 2004).

The possibility of GSC-specific endogenous NO synthesis remain unevaluated, and the contribution of other more targetable NOS isoforms to GSCs remains unexamined. Given the precedence that NO can support tumor growth and the aforementioned studies suggesting a pro-GSC effect for NO, we hypothesized that endogenous NO production might be augmented within GSCs relative to nonstem glioma cells (non-GSCs), thus promoting the established tumorigenic phenotype of GSCs.

RESULTS

Endogenous NO Contributes to Growth of GSCs, which Is Abrogated by Heterologous Expression of the Bacterial NO-Consuming Enzyme Flavohemoglobin

Employing techniques described in the Dirks group's original report first validating CD133 as a GSC cell surface marker (Singh et al., 2003), we characterized a variety of human tumor specimens and xenografts in which positive selection for CD133 segregates GSC-enriched populations from non-GSCs, as demonstrated by measures of self-renewal, stem cell marker expression, and tumor propagation potential (Bao et al., 2006a; Li et al., 2007). When CD133-based selection is utilized and stem cell-permissive culture conditions employed (Lee et al., 2006), CD133 marker expression is maintained (Figures S1A and S1B available online).

Using this CD133-based selection system, we compared the NO production capacity of CD133+ glioma cells (GSCs) with CD133– glioma cells (non-GSCs). We measured nitrite (NO_2^-), a stable byproduct of NO, in the culture medium using matched cultures from xenografted patient specimens. GSCs produced more NO_2^- than matched non-GSCs (Figure 1A), suggesting that elevated NO synthesis may be a distinctive feature of GSCs.

To examine the function of endogenous NO in GSCs, we designed and biochemically validated a strategy to deplete NO in mammalian cells (Forrester et al., 2011). While not conserved in mammals, bacteria and fungi employ flavohemoglobin (FlavoHb)—a potent NO-consuming enzyme that converts NO to nitrate (NO_3^-) (Figure 1B)—to protect from nitrosative stress (Gardner et al., 1998; Hausladen et al., 2001; Hausladen et al., 1998). Within GSCs and non-GSCs, we employed lentiviral-based expression of the *E. coli* FlavoHb. Efficient NO consumption by this approach was confirmed in HEK293 cells transfected with a CMV-driven NOS2, which results in supraphysiologic levels of NO (Figure 1C). Expression of FlavoHb impaired GSC growth (Figure 1D and Figure S1C) and neurosphere formation (Figure 1E and Figure S1D), though these effects were absent in CD133– non-GSCs and did not impact HEK293 cells that lack NO dependence (Figure S1E). Consumption of NO in GSCs via FlavoHb abrogated critical GSCs properties in vitro, suggesting a progrowth role for endogenous NO synthesis in GSCs.

Expression of NOS2 within GSCs Is Responsible for Their Distinctive NO Synthesis

While FlavoHb blocked NO availability and decreased GSC growth, the source of GSC-derived NO remained unclear. Glioma stem cells from primary patient specimens (Figure 2A) and human glioma xenografts (Figure 2B) displayed higher levels of NOS2 protein than matched non-GSCs, while no consistent expression pattern for NOS1 or NOS3 was observed. These data suggest that NOS2 expression in GSCs might contribute to their malignant properties, as (1) NOS2 is the most highly productive NOS, (2) *NOS2* is regulated largely at the level of transcription, and (3) GSCs demonstrated elevated endogenous NO production that contributed to GSC growth.

Although CD133 is useful for identifying GSCs (Bao et al., 2006a; Galli et al., 2004; Singh et al., 2003), it is not the only marker that may enrich for GSC phenotypes. The optimal method for defining GSC marker effectiveness likely depends on individual tumor characteristics and is a topic of active investigation. The marker stage-specific embryonic antigen-1 (SSEA1; CD15) has been reported to effectively isolate GSCs from some tumors with low CD133 expression (Son et al., 2009). Cell lysates from two of these previously reported tumors revealed elevated NOS2 expression in SSEA1+ GSCs relative to SSEA1– non-GSCs (Figure 2C). Positive selection for SSEA1 segregated for tumorigenic GSCs (as measured in transplantation assays) in these tumors from which we acquired SSEA1+ and SSEA1– protein lysates (Son et al., 2009). These data demonstrate that NOS2 cosegregates with GSC phenotypes in gliomas where CD133 or SSEA1 are useful for enriching GSCs.

To examine whether differential NOS2 expression is inadvertently driven by cell culture conditions, we used qRT-PCR to quantify *NOS2* messenger RNA (mRNA) derived from CD133+ and CD133– populations isolated by fluorescence-activated cell sorting (FACS) from fresh dissociated human gliomas
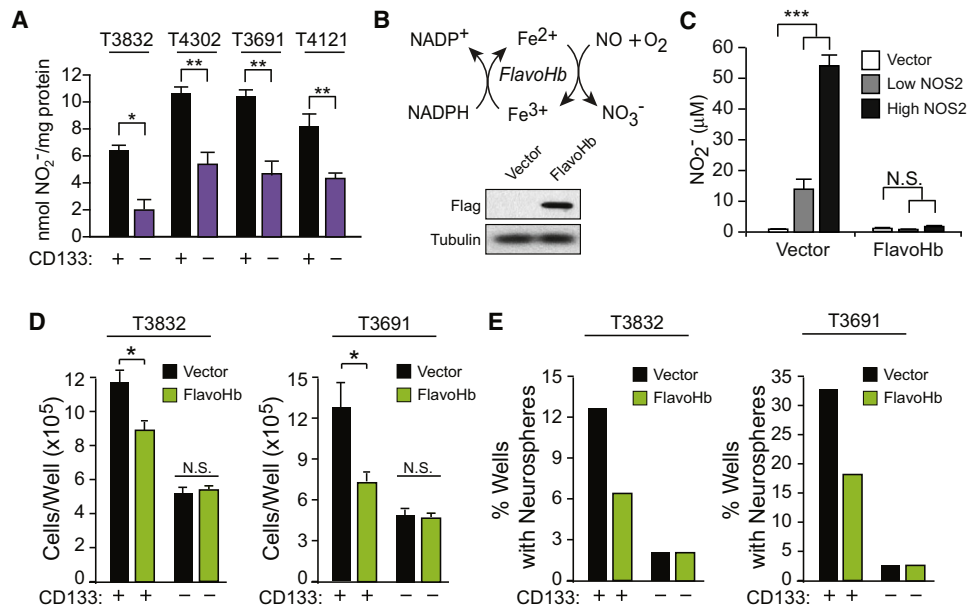
Figure 1. GSCs Synthesize NO, and Flavohemoglobin-Mediated NO Depletion Decreases GSC Growth

(A) Nitrite (NO_2^-) was quantified in the conditioned media of glioma xenografts (T3832, T4302, T3691, T4121) sorted into CD133+ (GSC) and CD133– (non-GSC) populations, and normalized to cellular protein.

(B) Microbial flavohemoglobin (FlavoHb) catalyzes the reaction of NO with oxygen to form inert nitrate (NO_3^-). A western blot verified Flag-tagged FlavoHb expression in GSCs.

(C) FlavoHb expression in NOS2-transfected HEK293 cells decreased the total NO_2^- measured in media, reflecting conversion of NO to NO_3^-.

(D and E) FlavoHb growth of xenograft-derived GSCs as measured by trypan blue exclusion (D) and GSC neurosphere formation capacity as measured 10 days after single cells were individually sorted into wells (E).

Scale bars represent 50 μm. N.S., not significant; *p < 0.05; **p < 0.01; ***p < 0.001. Error bars represent the mean ± standard error of the mean (SEM) of at least three measurements. See also Figure S1.

---

without intervening culture. Levels of *NOS2* mRNA were higher in GSCs relative to non-GSCs from three different primary human gliomas and a xenograft (Figure 2D). Previously described minor *NOS2* splice variants (Eissa et al., 1996, 1998; Tiscornia et al., 2004) were not detected in GSCs or non-GSCs (Figure S2A). Although these data indicate that full-length *NOS2* transcripts are elevated in GSCs in vivo, we further evaluated NOS2 protein and GSCs in human tissue. Immunofluorescence staining demonstrated coexpression of CD133 and NOS2 protein in human glioma tissue sections (Figure 2E and Figure S2B). Flow cytometry analysis of dissociated primary human glioma specimens showed that greater than 80% of NOS2-positive cells also express CD133 (Figure 2F). These findings collectively support the notion that NOS2 expression is elevated in GSCs.

To determine whether NOS2 is critical for GSC NO production, cells were treated with the highly selective NOS2 inhibitor 1400W (Garvey et al., 1997). Synthesis of NO was markedly attenuated in 1400W-treated GSCs, which had elevated NO production at baseline versus non-GSCs (Figure 2G and Figure S2C). Though in some tumors 1400W qualitatively decreased NO production in non-GSCs, this effect was less pronounced and not statistically significant in the setting of low overall NO production and minimal NOS2 expression in non-GSCs (Figure 2G).

Genetic or Pharmacologic Blockade of NOS2 Inhibits GSC Growth and Proliferation

Consumption of NO by FlavoHb blocked GSC growth and neurosphere formation (Figures 1D and 1E and Figures S1C and S1D) and NO production in GSCs was largely NOS2 dependent (Figure 2G). We therefore hypothesized that NOS2 activity in GSCs contributes to their known malignant properties. Short hairpin RNA (shRNA)-mediated knockdown of NOS2 (Figure 3A) resulted in decreased GSC growth and proliferation (Figures 3B–3D and Figures S3A–S3E) but had minimal effect on non-GSCs (Figures 3B–3D and Figures S3A, S3B, S3D, and S3E). Further, *NOS2*-directed shRNA decreased neurosphere formation in xenograft-derived GSCs (Figure 3E and Figure S3C). Neurospheres surviving *NOS2*-directed shRNA still expressed *NOS2* mRNA (assessed by qRT-PCR; data not shown) and thus were likely derived from cells that did not undergo *NOS2* knockdown or silenced *NOS2*-directed shRNA expression. Though FlavoHb does not affect the expression of NOS2 (Figure S3F), the antigrowth effect of *NOS2*-directed shRNA was comparable to results with FlavoHb-mediated NO consumption in GSCs (Figure S3G). Consistent with these results, the NOS2 inhibitor 1400W decreased GSC survival, proliferation, and neurosphere formation (Figures 3F–3H and Figures S3H–S3J), as did several other less-potent or less-selective NOS2 inhibitors (Figure S3K).
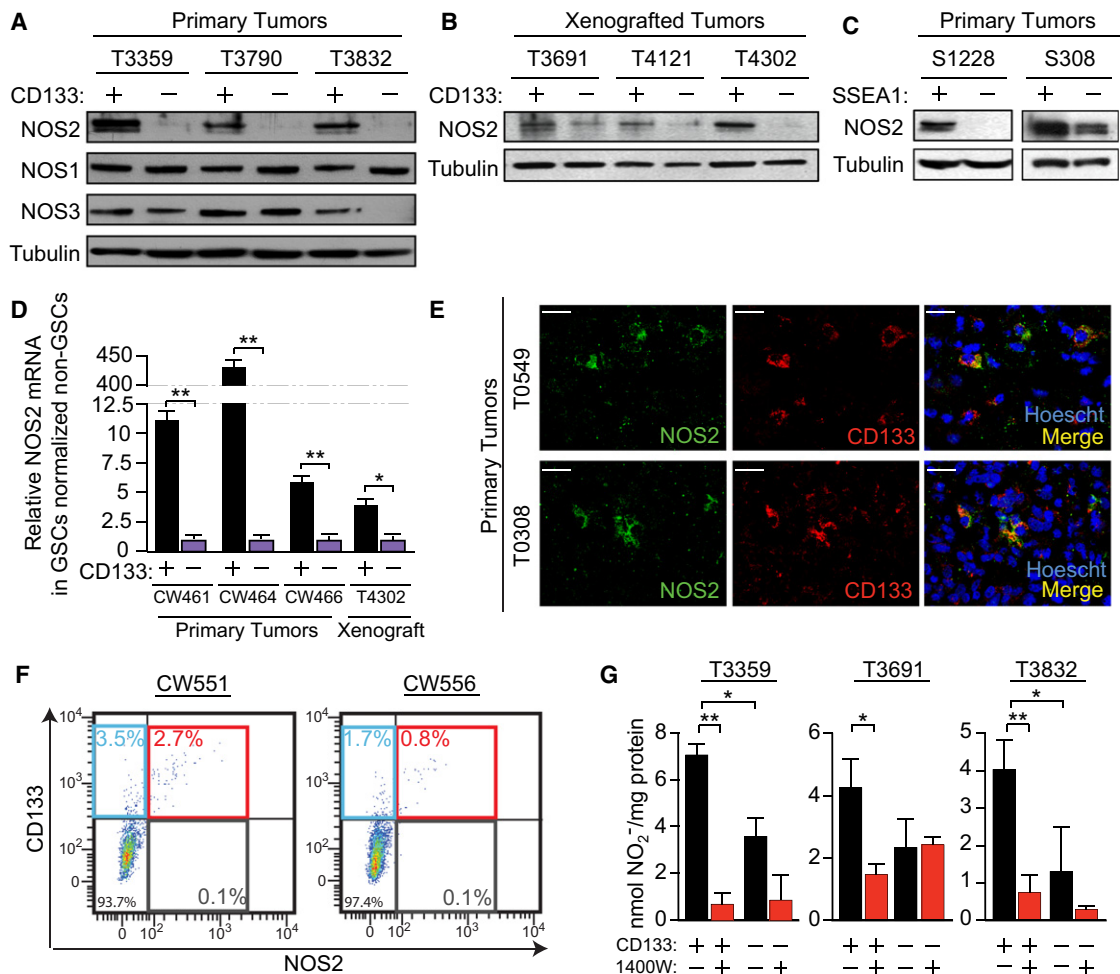
Figure 2. GSCs Selectively Express the NOS2 Isoform, which Is Primarily Responsible for Elevated NO Synthesis

(A and B) Western analysis of NOS2 expression in CD133+ cells (GSCs) versus CD133– cells (non-GSCs) in primary human specimens (A) and xenografted tumors (B).

(C) NOS2 expression levels were compared using western analysis in GSCs versus non-GSCs isolated via SSEA1-based sorting from S1228 and S308 tumors, for which SSEA1 has been previously validated as a functional marker of GSCs.

(D) GSCs and non-GSCs immediately isolated by FACS from fresh primary human brain tumors were analyzed for *NOS2* mRNA by qRT-PCR.

(E) Immunofluorescence of primary human tumor tissue sections revealed coexpression of CD133 and NOS2; scale bars represent 25 μm.

(F) Human primary malignant gliomas coexpressed NOS2 and CD133 via flow analysis performed immediately after isolation from fresh tissue.

(G) Media from xenograft-isolated cells with or without daily treatment with 100 μM 1400W was evaluated for NO_2^- levels, expressed as quantities normalized to total cellular protein.

$*p < 0.05$; $**p < 0.01$. Error bars represent the mean ± SEM of at least three measurements. See also Figure S2.

Targeting NOS2 Decreases Cell-Cycle Rate and Increases Expression of Cell Division Autoantigen 1

Due to the decreased growth of GSC populations after NOS2-directed interventions, we interrogated the rate of cell-cycle transit within individual GSCs using a 5-ethynyl-2′-deoxyuridine (EdU) incorporation assay. Both *NOS2*-directed shRNA and NOS2 inhibitor treatment decreased the rate of cell-cycle transit in GSCs (Figure 4A and Figures S4A and S4B), suggesting that endogenous NOS2 activity effects a proproliferative phenotype in GSCs.

We next screened for potential downstream molecular effectors of the proproliferative effects of GSC-specific NOS2 expres-

sion. We performed a microarray analysis of gene expression changes associated with *NOS2*-directed knockdown in human cells with endogenous NOS2 expression. Comparison of GSCs with or without *NOS2* knockdown revealed a variety of gene expression patterns altered by *NOS2*-directed shRNA treatment, and *NOS2* was one of the differentially represented genes, verifying successful knockdown (Table S1). Gene expression changes were further investigated by Ingenuity pathway analysis (Figures S4C and S4D).

Of the genes altered by *NOS2*-directed shRNA, we wanted to identify genes that were associated with human survival and with *NOS2* expression in the *Re*pository for *M*olecular *Bra*in
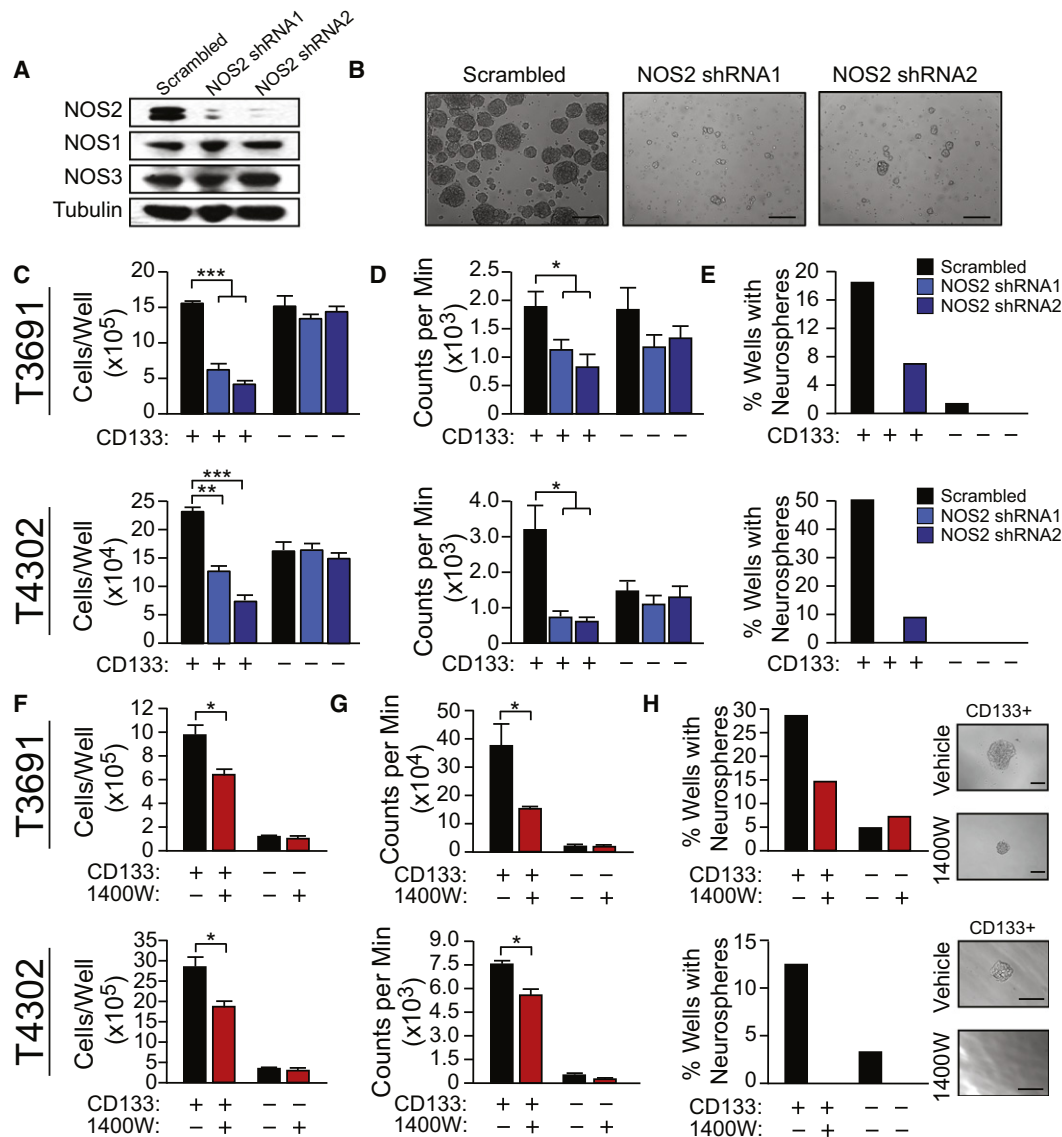
Figure 3. Knockdown or Inhibition of NOS2 Decreases GSC Growth and Neurosphere Formation

(A) Western analysis was employed to compare the selectivity of *NOS2*-directed shRNAs to NOS2 relative to NOS1 or NOS3 in T3691 CD133+ cells (GSCs).

(B) Representative images of neurospheres from (A); scale bars represent 50 μm.

(C and D) After *NOS2*-directed shRNA treatment of GSCs and CD133– cells (non-GSCs), (C) the number of viable cells were measured by trypan blue exclusion (C) and proliferation was measured by ^{3}H thymidine incorporation (D).

(E) Neurosphere formation after *NOS2*-directed shRNA treatment of GSCs was measured 10 days after single infected cells were individually sorted into wells.

(F–H) After inhibition of NOS2 with daily administration of 100 μM 1400W to GSCs and non-GSCs, the following were measured: viability by trypan blue exclusion (F), proliferation by ^{3}H thymidine incorporation (G), and neurosphere formation capacity (H). Representative images of neurospheres assessed in (H) are displayed; scale bars represent 50 μm.

*p < 0.05; **p < 0.01 ***p < 0.001. Error bars represent the mean ± SEM of at least three measurements. See also Figure S3.

*N*eoplasia *Dat*a (REMBRANDT) database (NCI, 2005). The REM-BRANDT database contains microarray-derived gene expression data from biopsies from 577 human patients with malignant glioma for which clinical outcome is known. The REMBRANDT database permits the retrospective analysis of each microarray-analyzed gene in the context of patient survival. Using this database, 49 of the *NOS2*-dependent probes identified in the microarray correlated with patient survival and 35 correlated with *NOS2* levels in the direction predicted by the microarray (Table S1). Only 11 probes satisfied both of these criteria, of which three were associated with the cell-cycle inhibitor cell division autoantigen 1 (*CDA1*, also known as *TSPYL2*). The only gene in the list with a known role in cell cycle or proliferation was *CDA1*. In the microarray studies, targeting of *NOS2* with directed shRNAs resulted in increased *CDA1* levels (Figure 4B). Although this is, to our knowledge, the first report of NO-
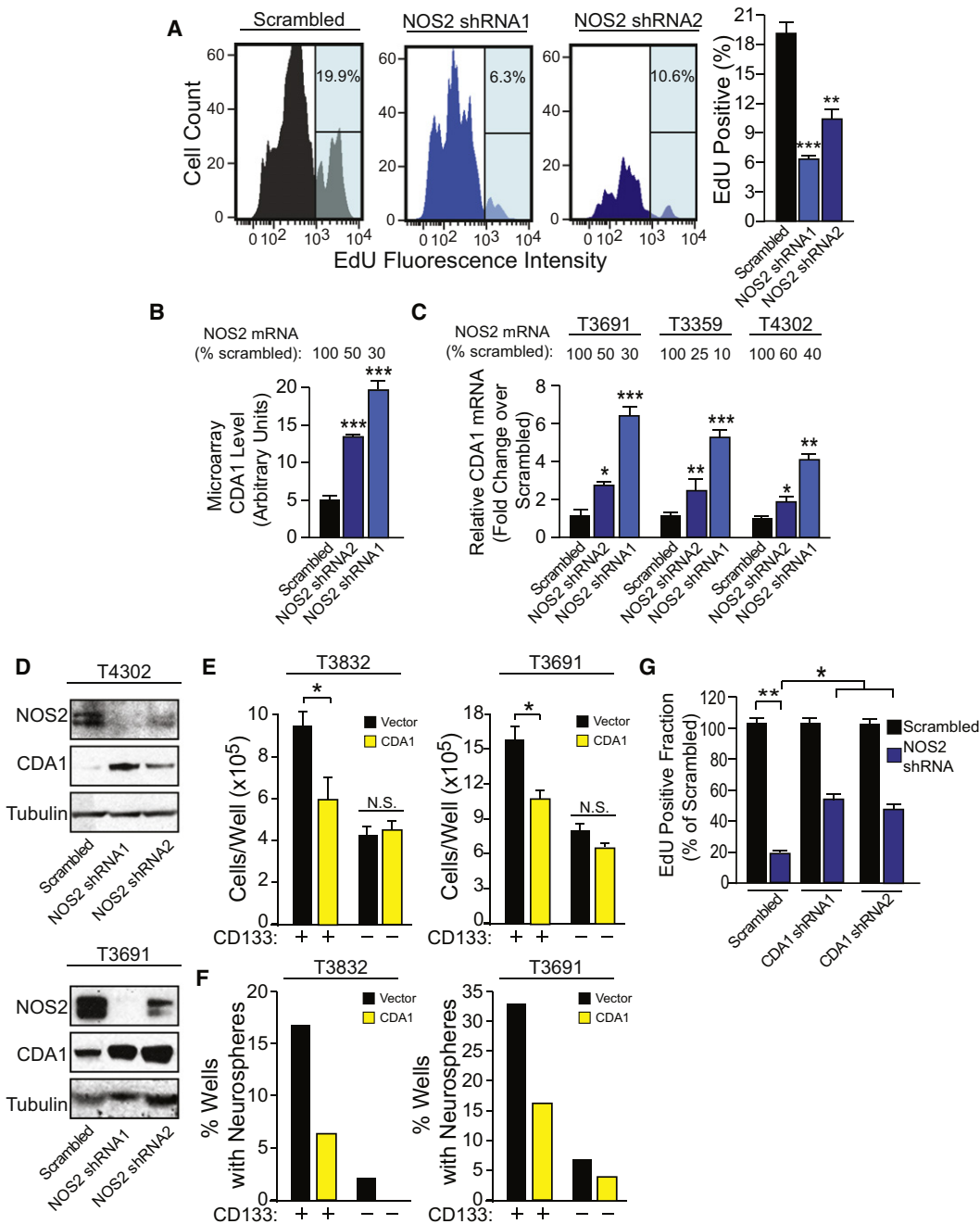
Figure 4. GSC Cell-Cycle Flux Is Supported by NOS2 Activity, which Modulates Gene Expression Including the Cell-Cycle Inhibitor *CDA1*

(A) 5-ethynyl-2′-deoxyuridine (EdU) incorporation assay was employed to evaluate the effect of *NOS2*-directed shRNA on S phase transit in CD133+ GSCs.

(B) Microarray analysis demonstrated that *NOS2*-directed shRNA increased transcript expression of the cell-cycle inhibitor, *CDA1* (two xenografts in duplicate).

(C and D) NOS2-dependent suppression of CDA1 in GSCs was validated by qRT-PCR (C) and western analysis (D).

(E) Viability of GSCs and CD133- cells (non-GSCs) was evaluated after treatment with vector or CDA1 expressing lentivirus.

(F) Neurosphere formation capacity was evaluated 10 d after single vector or CDA1-overexpressing cells were sorted into wells.

(G) The decreased EdU incorporation from *NOS2*-directed shRNAs was partially blocked by concurrent expression of *CDA1*-directed shRNA.

*p < 0.05; **p < 0.01; ***p < 0.001, N.S., not significant. Error bars represent the mean ± SEM of at least three measurements. See also Figure S4 and Table S1.

dependent repression of *CDA1*, this protein has previously been reported to be a pan-cell-cycle inhibitor and tumor suppressor, probably working through inhibition of multiple cyclin dependent kinases (Chai et al., 2001; Kandalaft et al., 2008; Tu et al., 2007). *NOS2*-dependent suppression of CDA1 was confirmed in several glioma xenografts by qRT-PCR (Figure 4C) and western

Figure 6. Normal Mouse and Human Neural Progenitor Cells Exhibit Minimal NOS2 Dependence

(A and B) Viability measured by trypan blue exclusion (A) and proliferation measured by ^{3}H thymidine incorporation (B) was evaluated in adult wild-type (WT) versus NOS2$^{-/-}$ mouse neural progenitor cells.

(C) Immunofluorescence was used to measure phospho-histone H3- (PH3; green) positive cells per field in the periventricular region of WT and NOS2$^{-/-}$ littermates. Dashed line, ventricular border. The scale bar represents 50 μm.

(D) Viability by trypan blue exclusion was measured in CD133+ cells (GSCs) and mouse neural progenitors with control or daily 100 μM 1400W treatment.

(E) Western analysis compared NOS2 expression in normal fetal NPCs (fNPCs) versus CD133+ GSCs and CD133– non-GSCs.

(F and G) *NOS2* mRNA levels were determined by qRT-PCR in fNPCs versus GSCs (F), and in human adult NPCs versus GSCs and non-GSCs from fresh primary gliomas immediately post-FACS isolation (G).

(H and I) CD133-mediated enrichment for the functional properties of GSCs in these tumors was validated with neurosphere formation. The effects of daily 1400W treatment on the viability of GSCs versus embryonic stem cell-derived NPCs (H) and two preparations of fNPCs (I).

examine the effects of NOS2 inhibitors in NPCs, we evaluated NPCs from mouse models, as well as human fetal and adult NPCs (Figure 6). Comparison of NPCs derived from wild-type (WT) and NOS2$^{-/-}$ mice revealed similar levels of cell growth and viability (Figures 6A and 6B). Similar levels of the proliferation marker phospho-histone H3 (PH3) were observed in the NPC-rich subependymal zone of WT and NOS2$^{-/-}$ adult mouse brains (Figure 6C). Since knockout mice may develop mechanisms by which they are able to compensate for the deletion of any given gene, we evaluated growth of WT mouse NPCs in response to acute administration of NOS2 inhibitor and observed no impact on growth (Figure 6D).

The potential role of NOS2 in normal NPCs was next analyzed in human cells. Normal human fetal NPCs (fNPCs) expressed markedly less NOS2 than GSCs (Figures 6E and 6F). Adult human NPCs isolated from normal human brain specimens also expressed less *NOS2* mRNA than xenograft-derived CD133+ GSCs (Figure S5A), as did CD133+ cells from primary human tumor specimens from which mRNA was harvested immediately after FACS sorting (i.e., without the influence of cell culture; Figure 6G). Inhibition of NOS2 had no growth impact on embryonic stem cell-derived NPCs (Figure 6H), nor did it affect the growth of two different fNPC preparations (Figure 6I). Unlike effects on GSCs, treatment with NOS2 inhibitor did not decrease neurosphere formation in fNPCs (Figure 6J). Human fNPCs and GSCs also have the capacity for multilineage differentiation, with GSCs being capable of aberrant differentiation (i.e., the expression of markers from multiple lineages in a single cell), also a known characteristic of GBM (Martinez-Diaz et al., 2003; Perry et al., 2009). However, NOS2 inhibition did not affect multilineage differentiation patterns in fNPCs or GSCs (Figures 6K and 6L and Figure S5B), suggesting that (1) NOS2 inhibition does not affect the differentiation potential of NPCs and (2) the anti-GSC effect of NOS2 inhibition does not relate to a promotion of differentiation. Together, these data suggest that NOS2-directed treatments would likely spare normal NPC growth and function, thus providing a favorable therapeutic margin for treating gliomas.

NOS2-Directed Interventions Decrease Glioma Growth In Vivo

Next, we sought to evaluate the potential antitumor effects of NOS2-directed interventions in vivo. First, we explored the relationship between cellular NO availability and tumor growth by implanting FlavoHb-expressing CD133+ GSCs into the brains of athymic mice, noting that consumption of cellular NO prolonged animal survival (Figure 7A). Next, to specifically evaluate the role of NOS2 expression within GSCs and tumorigenicity, we intracranially implanted *NOS2* shRNA-expressing GSCs into the forebrains of athymic mice. Consistent with results obtained with GSCs expressing the NO-consuming FlavoHb (Figure 7A), the time to development of neurological signs correlated with

the extent of *NOS2* knockdown (Figure 7B), suggesting that synthesis of NO by NOS2 contributes to the tumorigenicity of GSCs.

To translate our findings into a clinically relevant approach, we studied the antitumor activity of small molecule inhibitors against NOS2 in vivo. First, we examined the effects of the NOS2 inhibitor 1400W in mice bearing subcutaneous human glioma xenografts. Mice receiving 50 mg/kg of 1400W daily for 2 weeks had reduced tumor volumes compared to vehicle controls (Figure 7C). When tumors were excised after 17 days, overall tumor burden was markedly decreased by 1400W (Figure 7D), suggesting that NOS2 inhibitors have antiglioma effects in vivo. In these same tumors, there were indications of grossly decreased tumor angiogenesis as indicated by a decrease in vascularity (Figure 7C).

To confirm the efficacy of systemically administered NOS2 inhibitors using a more anatomically relevant model, we employed NOS2 inhibitors against intracranial glioma xenografts. The blood brain barrier (BBB), however, provides a formidable pharmacokinetic obstacle for charged or polar compounds such as the NOS2 inhibitor 1400W. Penetration of the BBB by 1400W is limited (Rebello et al., 2002), thus prompting the selection of alternative NOS2 inhibitors for BBB penetration (Figure S6A). The more lipophilic NOS2 inhibitor, BYK191023 (Strub et al., 2006), exhibited similar efficacy as 1400W for inhibition of CD133+ GSC growth in vitro (Figure S6B). However, BYK191023 possesses more suitable characteristics for BBB penetration, so it was therefore considered ideal for application in the intracranial glioma model. Luciferase-expressing glioma xenografts were implanted into the brains of athymic mice. After an engraftment period, tumor-bearing animals were randomly assigned to treatment groups. Mice treated with 60 mg/kg BYK191023 twice daily demonstrated significantly decreased tumor growth as measured by luminescence with two different patient-derived glioma xenografts in separate experiments (Figure 7E and Figure S6C). To assess whether these effects of NOS2 inhibition were related to GSCs, we dissociated control and BYK191023-treated tumors and evaluated cells for functional characteristics of GSCs. In vivo NOS2 inhibitor treatment decreased the ability of cells to form neurospheres (Figure S6D) and initiate secondary tumors in retransplantation assays (Figure S6E). Inhibitor-treated tumors therefore had fewer GSCs or GSCs with diminished self-renewal and tumorigenic capacity.

To more readily distinguish between requirements for NOS2 in tumor initiation or maintenance, we used an inducible *NOS2*-directed shRNA knockdown construct to deplete *NOS2* at implantation and then released shRNA induction to allow tumor growth with normal NOS2 expression levels. Transient knockdown during tumor engraftment did not affect overall tumor growth kinetics in vivo (Figure S6F). These data suggest that the effect of NOS2 activity in GSCs relates primarily to the maintenance, rather than the engraftment/initiation, of glioma.

(J) Neurosphere formation of GSCs versus fNPCs was quantified after 10 days of daily 1400W treatment.

(K and L) Multilineage differentiation capacity with vehicle or daily 1400W treatment in GSCs and fNPCs was evaluated by staining for astrocytic (GFAP), neuronal (Tuj1), and oligodendrocytic (O4) markers, shown as representative high power immunofluorescence images (K) and percent of marker positive cells per low power field (L); scale bars represent 10 μm.

*$p < 0.05$; **$p < 0.01$; ***$p < 0.001$. N.S., not significant. Error bars represent the mean ± SEM of at least three measurements. See also Figure S5.
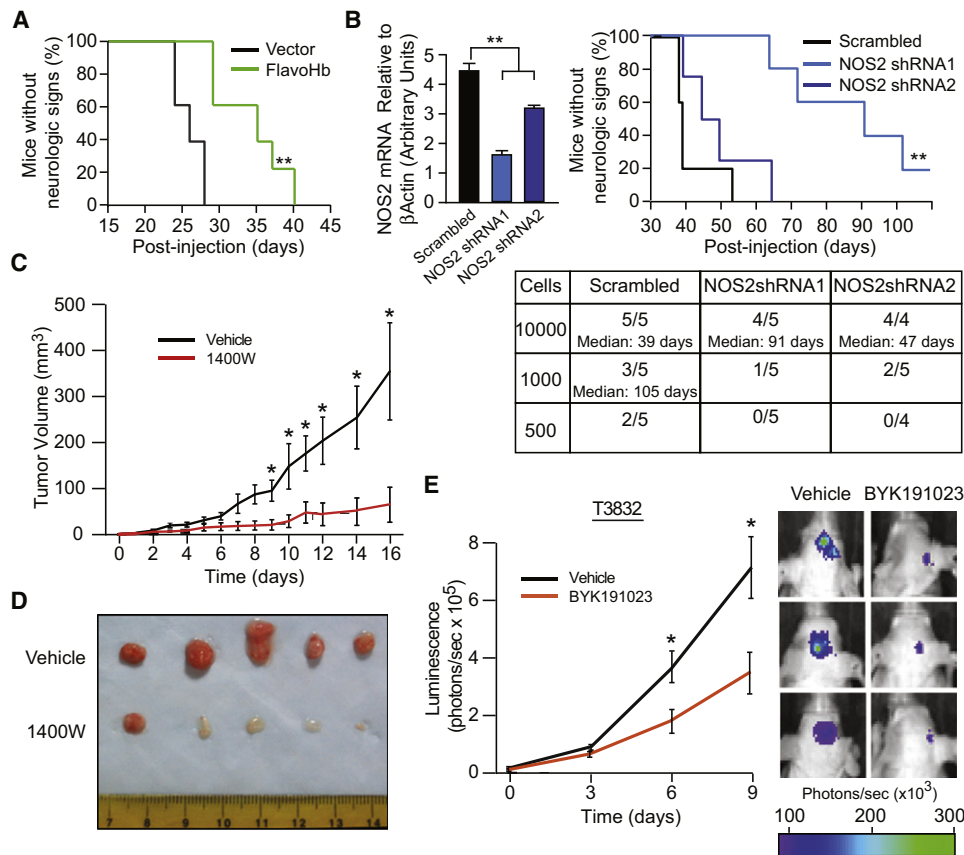
Figure 7. The Tumor Initiation and Maintenance Potential of GSCs Is Reduced by NO Depletion and NOS2 Knockdown/Inhibition

(A) Survival of athymic mice was tracked following intracranial implantation of 5000 CD133+ GSCs expressing either vector or FlavoHb.

(B) An intracranial in vivo limiting dilution survival assay (employing 10,000, 1000, and 500 cells per mouse) was performed using T3691 CD133+ cells, with qRT-PCR-verified *NOS2* knockdown. The table displays number of mice developing tumors and median time to neurologic signs. The survival curve displayed depicts mice injected with 10000 GSCs.

(C and D) Tumor volumes (C) and images of GSC derived subcutaneous xenografts (D) treated with daily intraperitoneal vehicle (n = 6) or 1400W (n = 6).

(E) T3832 luciferase-expressing GSC-derived intracranial xenografts treated with intraperitoneal vehicle or BYK191023 (n = 17 per group) after engraftment and tracked by bioluminescence. Real-time images from median three animals on day 9 are shown (right).

*p < 0.05; **p < 0.01. Error bars represent the mean ± SEM of the indicated number of animals. See also Figure S6.

No toxicities were observed in the mice treated with BYK191023, and BYK191023 was without effect on the slow-cycling subependymal neural progenitors in non-tumor-bearing mice (Figures S6G and S6H). Collectively, these data suggest that NOS2-directed therapeutics may represent a nontoxic and effective anti-GSC strategy with an effect primarily linked to tumor maintenance.

DISCUSSION

Here we demonstrate that NO synthesis, secondary to high NOS2 expression, is a distinctive feature of GSCs relative to non-GSCs and normal neural progenitors. Blockade of cellular NO availability with FlavoHb-based consumption or NOS2 inhibition/knockdown resulted in decreased GSC growth and tumorigenic capacity, suggesting an integral role for NO and endogenous NOS2 activity in the biology of GSCs. These findings are consistent with the wealth of reports showing that endogenously produced NO is generally cytoprotective (Rai et al., 1998; Sinz et al., 1999). In addition, systemic NOS2 inhibitors have been shown to block tumor growth (Thomsen et al., 1997), and NOS2 has an established cytoprotective role in chronic lymphocytic leukemia (Levesque et al., 2003; Zhao et al., 1998). Until our study, a role for CSC-synthesized NO has remained unexplored.

The molecular mechanisms by which NOS2 facilitates GSC proliferation and tumor growth are likely broad, as NO regulates a wide range of signaling pathways. The microarray analysis of GSCs treated with *NOS2*-directed shRNA knockdown suggests that NOS2 plays a role in regulating gene transcription of a variety of targets (Table S1) including suppression of the cell-cycle inhibitor *CDA1*, which has not previously been identified as an NO-regulated gene. Initiated by our microarray studies, we were able to determine that CDA1 repression mediates, at least in part, NO-mediated proliferation in GSCs. We provide evidence that NO likely represses overall transcription rates of *CDA1*, versus effects on CDA1 mRNA or protein stability (Figures S4F

and S4G). Further, it has previously been demonstrated that GSCs support tumor-mediated angiogenesis (Bao et al., 2006b), and our studies suggest a role for NOS2 as a proangiogenic factor in GSCs, as NOS2 inhibitor-treated tumors exhibited a gross decrease in blood vessels (Figure 7D). However, the contribution of NOS2 toward glioma angiogenesis remains a question for future study, while many other downstream targets for CSC-derived NO remain to be analyzed in the context of GSCs.

Previous studies have reported a role for NO in facilitating glioma cell growth (Lam-Himlin et al., 2006; Yamaguchi et al., 2002), and it has recently been suggested that NO synthesized by NOS3 (in the endothelium) or NOS1 (in glioma cells) may represent mechanisms by which the vasculature and neoplastic cells interact with each other to affect glioma growth and response to therapy (Charles et al., 2010; Kashiwagi et al., 2008). In particular, a recent publication (Charles et al., 2010) proposes a role for endothelium in promoting stem-like phenotypes in glioma cells in a PDGF-driven mouse model of glioma. Through in vitro administration of exogenous NO donors, they propose a role for NO (purportedly derived from the NOS3 activity in the vasculature in vivo) in the maintenance of GSC stem cell signaling. However, while their data do suggest that exogenous NO can promote certain CSC phenotypes, the source of this NO in vivo was never conclusively demonstrated beyond correlative staining. Further, even if endothelial NOS3 activity does play a role in sustaining GSCs, it is unlikely that NOS3-directed therapies will find clinical utility due to the negative impacts of inhibiting NOS3 in humans (Alexander et al., 2007; Avontuur et al., 1998; López et al., 2004). Finally, the side scatter-based method for isolating GSCs has recently been called into question as a valid technique for GSC isolation (Broadley et al., 2011).

Our report of NOS2 expression and activity within GSCs, however, is distinct from these previously identified roles for NO in glioma. This study identifies a cell-autonomous, GSC-specific source of NO, and it definitively highlights the expression and biological effects of the NOS2 isoform within GSCs using loss-of-function, multiple inhibitors, and NO consumption strategies. Moreover, our loss-of-function studies identify many genetic targets for NOS2 in GSCs (including the cell-cycle inhibitor protein CDA1), providing novel mechanistic information distinct from previous studies using exogenous NO donors. Finally, NOS2 inhibition may represent an antiglioma treatment option with an acceptably low toxicity profile, as demonstrated by the negligible toxicity of NOS2 inhibitor administration to humans (Brindicci et al., 2009; Dover et al., 2006; Singh et al., 2007).

We evaluated the toxicity of NOS2 inhibition on normal NPCs, and our results suggest nominal expression of NOS2 in normal NPCs as well as a minimal role for NOS2 in NPC growth. Our ability to fully assess the role of NOS2 in normal adult human NPCs was restricted by the lack of functionally validated established cell surface markers for human adult NPCs, so we could not assess NOS2 in NPCs acutely sorted from fresh human brain tissue. Thus, we utilized a strategy by which human adult neural stem cells are isolated by nestin-driven GFP via viral infection, which requires several days of cell culture. Cell culture has the capacity to select for cell populations or induce genetic or epigenetic changes in cells, and thus our studies of adult human NPCs are limited by the necessity of cell culture with these previously validated techniques (Keyoung et al., 2001).

Though one required characteristic of CSCs relates to their ability to generate tumors in transplantation assays, it is critical to realize that the molecular characteristics supporting the malignant characteristics of GSCs are not necessarily the same molecular alterations that permit transformation and thus generation of tumors de novo (Visvader, 2011). The antitumor effect of NOS2 inhibitors against engrafted tumors implies a role for NOS2 in the GSC-supported tumor maintenance. However, this does not mean that NOS2 is essential for the initial transformative event in tumors. In fact, our data suggest that the role of NOS2 relates primarily to tumor maintenance and not engraftment capacity.

We observed antitumor effects for 1400W and BYK191023 against glioma xenografts. Although 1400W effectively decreased subcutaneous tumor growth, it displayed limited efficacy against intracranial tumors (data not shown), probably as a result of the poor pharmacokinetic parameters of 1400W for intracranial delivery and BBB penetration (i.e., LogP = 0.71, cationic at neutral pH). The more lipophilic NOS2-selective inhibitor BYK191023, however, demonstrated effective antitumor activity against intracranial xenografts (Figure 7E). Though neither drug abolished tumor growth completely, both delayed tumor growth to a significant extent and may be useful when combined in multimodal treatment regimens that also target the tumor bulk.

BYK191023 could be a strong candidate for clinical evaluation as it possesses the following desirable characteristics: (1) it exhibits at least 1000-fold selectivity for NOS2 over NOS1 and NOS3 (Strub et al., 2006), (2) it adheres to "Lipinski's rules of five" for optimal pharmacokinetics and bioavailability (Lipinski et al., 2001), (3) it is sufficiently lipophilic for BBB penetration (i.e., LogP 1.84), and (4) it decreases GSC growth and survival in vitro and in vivo. In combination with the minimal toxic potential for NOS2 inhibition in humans and the effective anti-GSC activity demonstrated in our investigations, the data provided here will hopefully serve as an impetus for evaluation of NOS2-directed therapies as a component of multimodal treatment regimens for human glioma.

EXPERIMENTAL PROCEDURES

Isolation and Culture of GSCs and Non-GSCs from Xenografts and Primary Human Specimens
GSCs and non-GSCs were isolated from tumor tissue or xenografts (Table S2) as previously described (Bao et al., 2006a; Li et al., 2009).

Nitrite Level Determination by 4,5-Diaminofluorescein
For determination of cellular nitrite production, conditioned supernatants or nitrite standards were added to 4,5-diaminofluorescein (DAF-2; Cayman Chemical) (Kojima et al., 1998; Nakatsubo et al., 1998). Samples were analyzed postacidification and neutralization for fluorescence measured with $\lambda ex = 488$ nm and $\lambda em = 525$ nm, and the results were normalized to cellular protein content (measured by Bradford assay; Bio-Rad).

Neurosphere Formation Assay
Neurosphere formation assays were performed in a manner similar to our prior report (Li et al., 2009), with propidium iodide-negative cells sorted by FACS to

a single cells per well of 96-well plates. For NOS2 inhibitor studies, vehicle or 100 μM 1400W was added daily. Neurosphere formation was measured as the percent of wells with neurospheres after 10 days.

Assessment of In Vivo Glioma Progression after Treatment with NOS2 Inhibitors, *NOS2* Knockdown, and Flavohemoglobin

For bioluminescence imaging, GSCs stably expressing firefly luciferase were intracranially injected into the right forebrains of 4- to 6-week-old athymic nude mice, and the Xenogen system was used for imaging every 3 days. Survival studies were performed as in our prior report (Li et al., 2009), with intracranial injection of lentivirally infected CD133+ cells. Mice were monitored daily until the development of neurological or constitutional signs (e.g., ataxia, lethargy, and seizures).

Retrospective Analysis of *NOS2* and *CDA1* Expression in Human Gliomas

The National Cancer Institute's Repository for Molecular Brain Neoplasia Data (REMBRANDT, http://rembrandt.nci.nih.gov/, accessed 6/25/10) was evaluated for correlations between clinical outcome/survival and gene expression in malignant glioma biopsies. For REMBRANDT, "upregulated" is defined as expression >2.0-fold relative to mean values in normal tissue, whereas "downregulated" is defined as expression <0.5-fold relative to mean values in normal tissue. "Intermediate" expression is the range between "upregulated" and "downregulated" (i.e., between 0.5- and 2-fold relative to mean values in normal tissue).

Microarray Expression Analysis of *NOS2* Knockdown in CD133+ GSCs

CD133+ cells derived from two different xenografts (T3359 and T3691) were treated in duplicate for 72 hr with either nontargeting scramble control shRNA or two distinct *NOS2*-directed shRNAs. Total RNA was harvested, reverse transcribed, labeled, and hybridized to Illumina BeadArrays. BeadStudio software was used to normalize scanned chip data and to subtract background signal, and chip effects were removed by ANOVA.

ACCESSION NUMBERS

The GEO accession number for the microarray expression analysis of *NOS2* knockdown in GSCs reported in this paper is GSE29750.

SUPPLEMENTAL INFORMATION

Supplemental Information includes Extended Experimental Procedures, six figures, and three tables and can be found with this article online at doi:10.1016/j.cell.2011.06.006.

REFERENCES

Alexander, J.H., Reynolds, H.R., Stebbins, A.L., Dzavik, V., Harrington, R.A., Van de Werf, F., and Hochman, J.S.; TRIUMPH Investigators. (2007). Effect of tilarginine acetate in patients with acute myocardial infarction and cardiogenic shock: the TRIUMPH randomized controlled trial. JAMA 297, 1657–1666.

Androutsellis-Theotokis, A., Leker, R.R., Soldner, F., Hoeppner, D.J., Ravin, R., Poser, S.W., Rueger, M.A., Bae, S.K., Kittappa, R., and McKay, R.D. (2006). Notch signalling regulates stem cell numbers in vitro and in vivo. Nature 442, 823–826.

Avontuur, J.A., Tutein Nolthenius, R.P., van Bodegom, J.W., and Bruining, H.A. (1998). Prolonged inhibition of nitric oxide synthesis in severe septic shock: a clinical study. Crit. Care Med. 26, 660–667.

Bakshi, A., Nag, T.C., Wadhwa, S., Mahapatra, A.K., and Sarkar, C. (1998). The expression of nitric oxide synthases in human brain tumours and peritumoral areas. J. Neurol. Sci. 155, 196–203.

Bao, S., Wu, Q., McLendon, R.E., Hao, Y., Shi, Q., Hjelmeland, A.B., Dewhirst, M.W., Bigner, D.D., and Rich, J.N. (2006a). Glioma stem cells promote radioresistance by preferential activation of the DNA damage response. Nature 444, 756–760.

Bao, S., Wu, Q., Sathornsumetee, S., Hao, Y., Li, Z., Hjelmeland, A.B., Shi, Q., McLendon, R.E., Bigner, D.D., and Rich, J.N. (2006b). Stem cell-like glioma cells promote tumor angiogenesis through vascular endothelial growth factor. Cancer Res. 66, 7843–7848.

Bar, E.E., Chaudhry, A., Lin, A., Fan, X., Schreck, K., Matsui, W., Piccirillo, S., Vescovi, A.L., DiMeco, F., Olivi, A., and Eberhart, C.G. (2007). Cyclopamine-mediated hedgehog pathway inhibition depletes stem-like cancer cells in glioblastoma. Stem Cells 25, 2524–2533.

Ben-Porath, I., Thomson, M.W., Carey, V.J., Ge, R., Bell, G.W., Regev, A., and Weinberg, R.A. (2008). An embryonic stem cell-like gene expression signature in poorly differentiated aggressive human tumors. Nat. Genet. 40, 499–507.

Bonnet, D., and Dick, J.E. (1997). Human acute myeloid leukemia is organized as a hierarchy that originates from a primitive hematopoietic cell. Nat. Med. 3, 730–737.

Brindicci, C., Ito, K., Torre, O., Barnes, P.J., and Kharitonov, S.A. (2009). Effects of aminoguanidine, an inhibitor of inducible nitric oxide synthase, on nitric oxide production and its metabolites in healthy control subjects, healthy smokers, and COPD patients. Chest 135, 353–367.

Broadley, K.W., Hunn, M.K., Farrand, K.J., Price, K.M., Grasso, C., Miller, R.J., Hermans, I.F., and McConnell, M.J. (2011). Side population is not necessary or sufficient for a cancer stem cell phenotype in glioblastoma multiforme. Stem Cells 29, 452–461.

Chai, Z., Sarcevic, B., Mawson, A., and Toh, B.H. (2001). SET-related cell division autoantigen-1 (CDA1) arrests cell growth. J. Biol. Chem. 276, 33665–33674.

Charles, N., Ozawa, T., Squatrito, M., Bleau, A.M., Brennan, C.W., Hambardzumyan, D., and Holland, E.C. (2010). Perivascular nitric oxide activates notch signaling and promotes stem-like character in PDGF-induced glioma cells. Cell Stem Cell 6, 141–152.

Clement, V., Sanchez, P., de Tribolet, N., Radovanovic, I., and Ruiz i Altaba, A. (2007). HEDGEHOG-GLI1 signaling regulates human glioma growth, cancer stem cell self-renewal, and tumorigenicity. Curr. Biol. 17, 165–172.

Cobbs, C.S., Brenman, J.E., Aldape, K.D., Bredt, D.S., and Israel, M.A. (1995). Expression of nitric oxide synthase in human central nervous system tumors. Cancer Res. 55, 727–730.

Dover, A.R., Chia, S., Ferguson, J.W., Cruden, N.L., Megson, I.L., Fox, K.A., and Newby, D.E. (2006). Inducible nitric oxide synthase activity does not

contribute to the maintenance of peripheral vascular tone in patients with heart failure. Clin. Sci. *111*, 275–280.

Eissa, N.T., Strauss, A.J., Haggerty, C.M., Choo, E.K., Chu, S.C., and Moss, J. (1996). Alternative splicing of human inducible nitric-oxide synthase mRNA. tissue-specific regulation and induction by cytokines. J. Biol. Chem. *271*, 27184–27187.

Eissa, N.T., Yuan, J.W., Haggerty, C.M., Choo, E.K., Palmer, C.D., and Moss, J. (1998). Cloning and characterization of human inducible nitric oxide synthase splice variants: a domain, encoded by exons 8 and 9, is critical for dimerization. Proc. Natl. Acad. Sci. USA *95*, 7625–7630.

Engels, K., Knauer, S.K., Loibl, S., Fetz, V., Harter, P., Schweitzer, A., Fisseler-Eckhoff, A., Kommoss, F., Hanker, L., Nekljudova, V., et al. (2008). NO signaling confers cytoprotectivity through the survivin network in ovarian carcinomas. Cancer Res. *68*, 5159–5166.

Fan, X., Matsui, W., Khaki, L., Stearns, D., Chun, J., Li, Y.M., and Eberhart, C.G. (2006). Notch pathway inhibition depletes stem-like cells and blocks engraftment in embryonal brain tumors. Cancer Res. *66*, 7445–7452.

Fetz, V., Bier, C., Habtemichael, N., Schuon, R., Schweitzer, A., Kunkel, M., Engels, K., Kovács, A.F., Schneider, S., Mann, W., et al. (2009). Inducible NO synthase confers chemoresistance in head and neck cancer by modulating survivin. Int. J. Cancer *124*, 2033–2041.

Forrester, M.T., Eyler, C.E., and Rich, J.N. (2011). Bacterial flavohemoglobin: a molecular tool to probe mammalian nitric oxide biology. Biotechniques *50*, 41–45.

Fukumura, D., Kashiwagi, S., and Jain, R.K. (2006). The role of nitric oxide in tumour progression. Nat. Rev. Cancer *6*, 521–534.

Galli, R., Binda, E., Orfanelli, U., Cipelletti, B., Gritti, A., De Vitis, S., Fiocco, R., Foroni, C., Dimeco, F., and Vescovi, A. (2004). Isolation and characterization of tumorigenic, stem-like neural precursors from human glioblastoma. Cancer Res. *64*, 7011–7021.

Gardner, P.R., Gardner, A.M., Martin, L.A., and Salzman, A.L. (1998). Nitric oxide dioxygenase: an enzymic function for flavohemoglobin. Proc. Natl. Acad. Sci. USA *95*, 10378–10383.

Garvey, E.P., Oplinger, J.A., Furfine, E.S., Kiff, R.J., Laszlo, F., Whittle, B.J., and Knowles, R.G. (1997). 1400W is a slow, tight binding, and highly selective inhibitor of inducible nitric-oxide synthase in vitro and in vivo. J. Biol. Chem. *272*, 4959–4963.

Hausladen, A., Gow, A.J., and Stamler, J.S. (1998). Nitrosative stress: metabolic pathway involving the flavohemoglobin. Proc. Natl. Acad. Sci. USA *95*, 14100–14105.

Hausladen, A., Gow, A., and Stamler, J.S. (2001). Flavohemoglobin denitrosylase catalyzes the reaction of a nitroxyl equivalent with molecular oxygen. Proc. Natl. Acad. Sci. USA *98*, 10108–10112.

Iadecola, C., Zhang, F., Casey, R., Nagayama, M., and Ross, M.E. (1997). Delayed reduction of ischemic brain injury and neurological deficits in mice lacking the inducible nitric oxide synthase gene. J. Neurosci. *17*, 9157–9164.

Kandalaft, L.E., Zudaire, E., Portal-Núñez, S., Cuttitta, F., and Jakowlew, S.B. (2008). Differentially expressed nucleolar transforming growth factor-beta1 target (DENTT) exhibits an inhibitory role on tumorigenesis. Carcinogenesis *29*, 1282–1289.

Kashiwagi, S., Tsukada, K., Xu, L., Miyazaki, J., Kozin, S.V., Tyrrell, J.A., Sessa, W.C., Gerweck, L.E., Jain, R.K., and Fukumura, D. (2008). Perivascular nitric oxide gradients normalize tumor vasculature. Nat. Med. *14*, 255–257.

Keyoung, H.M., Roy, N.S., Benraiss, A., Louissaint, A., Jr., Suzuki, A., Hashimoto, M., Rashbaum, W.K., Okano, H., and Goldman, S.A. (2001). High-yield selection and extraction of two promoter-defined phenotypes of neural stem cells from the fetal human brain. Nat. Biotechnol. *19*, 843–850.

Kojima, H., Nakatsubo, N., Kikuchi, K., Kawahara, S., Kirino, Y., Nagoshi, H., Hirata, Y., and Nagano, T. (1998). Detection and imaging of nitric oxide with novel fluorescent indicators: diaminofluoresceins. Anal. Chem. *70*, 2446–2453.

Lam-Himlin, D., Espey, M.G., Perry, G., Smith, M.A., and Castellani, R.J. (2006). Malignant glioma progression and nitric oxide. Neurochem. Int. *49*, 764–768.

Lapidot, T., Sirard, C., Vormoor, J., Murdoch, B., Hoang, T., Caceres-Cortes, J., Minden, M., Paterson, B., Caligiuri, M.A., and Dick, J.E. (1994). A cell initiating human acute myeloid leukaemia after transplantation into SCID mice. Nature *367*, 645–648.

Lee, J., Kotliarova, S., Kotliarov, Y., Li, A., Su, Q., Donin, N.M., Pastorino, S., Purow, B.W., Christopher, N., Zhang, W., et al. (2006). Tumor stem cells derived from glioblastomas cultured in bFGF and EGF more closely mirror the phenotype and genotype of primary tumors than do serum-cultured cell lines. Cancer Cell *9*, 391–403.

Levesque, M.C., Misukonis, M.A., O'Loughlin, C.W., Chen, Y., Beasley, B.E., Wilson, D.L., Adams, D.J., Silber, R., and Weinberg, J.B. (2003). IL-4 and interferon gamma regulate expression of inducible nitric oxide synthase in chronic lymphocytic leukemia cells. Leukemia *17*, 442–450.

Li, F., Sonveaux, P., Rabbani, Z.N., Liu, S., Yan, B., Huang, Q., Vujaskovic, Z., Dewhirst, M.W., and Li, C.Y. (2007). Regulation of HIF-1alpha stability through S-nitrosylation. Mol. Cell *26*, 63–74.

Li, Z., Bao, S., Wu, Q., Wang, H., Eyler, C., Sathornsumetee, S., Shi, Q., Cao, Y., Lathia, J., McLendon, R.E., et al. (2009). Hypoxia-inducible factors regulate tumorigenic capacity of glioma stem cells. Cancer Cell *15*, 501–513.

Lim, K.H., Ancrile, B.B., Kashatus, D.F., and Counter, C.M. (2008). Tumour maintenance is mediated by eNOS. Nature *452*, 646–649.

Lipinski, C.A., Lombardo, F., Dominy, B.W., and Feeney, P.J. (2001). Experimental and computational approaches to estimate solubility and permeability in drug discovery and development settings. Adv. Drug Deliv. Rev. *46*, 3–26.

López, A., Lorente, J.A., Steingrub, J., Bakker, J., McLuckie, A., Willatts, S., Brockway, M., Anzueto, A., Holzapfel, L., Breen, D., et al. (2004). Multiple-center, randomized, placebo-controlled, double-blind study of the nitric oxide synthase inhibitor 546C88: effect on survival in patients with septic shock. Crit. Care Med. *32*, 21–30.

Luo, C.X., Zhu, X.J., Zhou, Q.G., Wang, B., Wang, W., Cai, H.H., Sun, Y.J., Hu, M., Jiang, J., Hua, Y., et al. (2007). Reduced neuronal nitric oxide synthase is involved in ischemia-induced hippocampal neurogenesis by up-regulating inducible nitric oxide synthase expression. J. Neurochem. *103*, 1872–1882.

MacMicking, J.D., Nathan, C., Hom, G., Chartrain, N., Fletcher, D.S., Trumbauer, M., Stevens, K., Xie, Q.W., Sokol, K., Hutchinson, N., et al. (1995). Altered responses to bacterial infection and endotoxic shock in mice lacking inducible nitric oxide synthase. Cell *81*, 641–650.

Martinez-Diaz, H., Kleinschmidt-DeMasters, B.K., Powell, S.Z., and Yachnis, A.T. (2003). Giant cell glioblastoma and pleomorphic xanthoastrocytoma show different immunohistochemical profiles for neuronal antigens and p53 but share reactivity for class III beta-tubulin. Arch. Pathol. Lab. Med. *127*, 1187–1191.

Nakatsubo, N., Kojima, H., Kikuchi, K., Nagoshi, H., Hirata, Y., Maeda, D., Imai, Y., Irimura, T., and Nagano, T. (1998). Direct evidence of nitric oxide production from bovine aortic endothelial cells using new fluorescence indicators: diaminofluoresceins. FEBS Lett. *427*, 263–266.

NCI. (2005). National Cancer Institute REMBRANDT home page. http://rembrandt.nci.nih.gov, accessed 2010 June 25.

Perry, A., Miller, C.R., Gujrati, M., Scheithauer, B.W., Zambrano, S.C., Jost, S.C., Raghavan, R., Qian, J., Cochran, E.J., Huse, J.T., et al. (2009). Malignant gliomas with primitive neuroectodermal tumor-like components: a clinicopathologic and genetic study of 53 cases. Brain Pathol. *19*, 81–90.

Rai, R.M., Lee, F.Y., Rosen, A., Yang, S.Q., Lin, H.Z., Koteish, A., Liew, F.Y., Zaragoza, C., Lowenstein, C., and Diehl, A.M. (1998). Impaired liver regeneration in inducible nitric oxide synthasedeficient mice. Proc. Natl. Acad. Sci. USA *95*, 13829–13834.

Rebello, S.S., Zhu, B., McMonagle-Strucko, K., Pulicicchio, C., Merrill, J., Luo, Y., Shen, L., Wang, J., Adler, D., and Natarajan, C. (2002). Pharmacokinetic and pharmacodynamic evaluation of inhibitors of inducible nitric oxide

synthase (iNOS) in mice. AAPS PharmSci *4* (*S1*). http://www.aapsj.org/abstracts/AM_2002/AAPS2002-002237.pdf.

Reya, T., Morrison, S.J., Clarke, M.F., and Weissman, I.L. (2001). Stem cells, cancer, and cancer stem cells. Nature *414*, 105–111.

Reya, T., Duncan, A.W., Ailles, L., Domen, J., Scherer, D.C., Willert, K., Hintz, L., Nusse, R., and Weissman, I.L. (2003). A role for Wnt signalling in self-renewal of haematopoietic stem cells. Nature *423*, 409–414.

Shackleton, M., Quintana, E., Fearon, E.R., and Morrison, S.J. (2009). Heterogeneity in cancer: cancer stem cells versus clonal evolution. Cell *138*, 822–829.

Singh, S.K., Clarke, I.D., Terasaki, M., Bonn, V.E., Hawkins, C., Squire, J., and Dirks, P.B. (2003). Identification of a cancer stem cell in human brain tumors. Cancer Res. *63*, 5821–5828.

Singh, D., Richards, D., Knowles, R.G., Schwartz, S., Woodcock, A., Langley, S., and O'Connor, B.J. (2007). Selective inducible nitric oxide synthase inhibition has no effect on allergen challenge in asthma. Am. J. Respir. Crit. Care Med. *176*, 988–993.

Sinz, E.H., Kochanek, P.M., Dixon, C.E., Clark, R.S., Carcillo, J.A., Schiding, J.K., Chen, M., Wisniewski, S.R., Carlos, T.M., Williams, D., et al. (1999). Inducible nitric oxide synthase is an endogenous neuroprotectant after traumatic brain injury in rats and mice. J. Clin. Invest. *104*, 647–656.

Son, M.J., Woolard, K., Nam, D.H., Lee, J., and Fine, H.A. (2009). SSEA-1 is an enrichment marker for tumor-initiating cells in human glioblastoma. Cell Stem Cell *4*, 440–452.

Strub, A., Ulrich, W.R., Hesslinger, C., Eltze, M., Fuchss, T., Strassner, J., Strand, S., Lehner, M.D., and Boer, R. (2006). The novel imidazopyridine 2-[2-(4-methoxy-pyridin-2-yl)-ethyl]-3H-imidazo[4,5-b]pyridine (BYK191023) is a highly selective inhibitor of the inducible nitric-oxide synthase. Mol. Pharmacol. *69*, 328–337.

Stupp, R., Mason, W.P., van den Bent, M.J., Weller, M., Fisher, B., Taphoorn, M.J., Belanger, K., Brandes, A.A., Marosi, C., Bogdahn, U., et al; European Organisation for Research and Treatment of Cancer Brain Tumor and Radiotherapy Groups; National Cancer Institute of Canada Clinical Trials Group. (2005). Radiotherapy plus concomitant and adjuvant temozolomide for glioblastoma. N. Engl. J. Med. *352*, 987–996.

Taylor, M.D., Poppleton, H., Fuller, C., Su, X., Liu, Y., Jensen, P., Magdaleno, S., Dalton, J., Calabrese, C., Board, J., et al. (2005). Radial glia cells are candidate stem cells of ependymoma. Cancer Cell *8*, 323–335.

Thomsen, L.L., Scott, J.M., Topley, P., Knowles, R.G., Keerie, A.J., and Frend, A.J. (1997). Selective inhibition of inducible nitric oxide synthase inhibits tumor growth in vivo: studies with 1400W, a novel inhibitor. Cancer Res. *57*, 3300–3304.

Tiscornia, A.C., Cayota, A., Landoni, A.I., Brito, C., Oppezzo, P., Vuillier, F., Robello, C., Dighiero, G., Gabús, R., and Pritsch, O. (2004). Post-transcriptional regulation of inducible nitric oxide synthase in chronic lymphocytic leukemia B cells in pro- and antiapoptotic culture conditions. Leukemia *18*, 48–56.

Tu, Y., Wu, W., Wu, T., Cao, Z., Wilkins, R., Toh, B.H., Cooper, M.E., and Chai, Z. (2007). Antiproliferative autoantigen CDA1 transcriptionally up-regulates p21(Waf1/Cip1) by activating p53 and MEK/ERK1/2 MAPK pathways. J. Biol. Chem. *282*, 11722–11731.

Visvader, J.E. (2011). Cells of origin in cancer. Nature *469*, 314–322.

Wechsler-Reya, R.J., and Scott, M.P. (1999). Control of neuronal precursor proliferation in the cerebellum by Sonic Hedgehog. Neuron *22*, 103–114.

Wei, X.Q., Charles, I.G., Smith, A., Ure, J., Feng, G.J., Huang, F.P., Xu, D., Muller, W., Moncada, S., and Liew, F.Y. (1995). Altered immune responses in mice lacking inducible nitric oxide synthase. Nature *375*, 408–411.

Williams, E.L., and Djamgoz, M.B. (2005). Nitric oxide and metastatic cell behaviour. Bioessays *27*, 1228–1238.

Yamaguchi, S., Bell, H.S., Shinoda, J., Holmes, M.C., Wharton, S.B., and Whittle, I.R. (2002). Glioma tumourgenicity is decreased by iNOS knockout: experimental studies using the C6 striatal implantation glioma model. Br. J. Neurosurg. *16*, 567–572.

Yang, D.I., Yin, J.H., Mishra, S., Mishra, R., and Hsu, C.Y. (2002). NO-mediated chemoresistance in C6 glioma cells. Ann. N Y Acad. Sci. *962*, 8–17.

Yilmaz, O.H., Valdez, R., Theisen, B.K., Guo, W., Ferguson, D.O., Wu, H., and Morrison, S.J. (2006). Pten dependence distinguishes haematopoietic stem cells from leukaemia-initiating cells. Nature *441*, 475–482.

Yuan, X., Curtin, J., Xiong, Y., Liu, G., Waschsmann-Hogiu, S., Farkas, D.L., Black, K.L., and Yu, J.S. (2004). Isolation of cancer stem cells from adult glioblastoma multiforme. Oncogene *23*, 9392–9400.

Zhao, H., Dugas, N., Mathiot, C., Delmer, A., Dugas, B., Sigaux, F., and Kolb, J.P. (1998). B-cell chronic lymphocytic leukemia cells express a functional inducible nitric oxide synthase displaying anti-apoptotic activity. Blood *92*, 1031–1043.

Zhao, X., Haensel, C., Araki, E., Ross, M.E., and Iadecola, C. (2000). Gene-dosing effect and persistence of reduction in ischemic brain injury in mice lacking inducible nitric oxide synthase. Brain Res. *872*, 215–218.